Quantum interference in resonance fluorescence for a driven V atom

Peng Zhou* and S. Swain†
Department of Applied Mathematics and Theoretical Physics, The Queen's University of Belfast, Belfast BT7 1NN, United Kingdom
(Received 19 May 1997)

We investigate the effect of quantum interference between the two transition pathways from the excited doublet to the ground level of a driven V atom on the spectral features of the resonance fluorescence emission. The ultranarrow spectral line at line center, which arises due to quantum interference, occurs over a wide range of parameters. The smaller the ratio of the excited doublet splitting to the effective Rabi frequency, the more pronounced the spectral line narrowing. However, the fluorescence emission is completely quenched when the atomic dipole moments are exactly parallel and the driving field is tuned to the average frequency of the atomic transitions. The narrow line is due to the slow decay rate of one dressed state, while the quenching arises from dressed-state trapping. A finite laser linewidth destroys the spectral narrowing features and the fluorescence quenching. [S1050-2947(97)07509-4]

PACS number(s): 32.80.Bx, 42.50.Gy, 42.50.Lc

I. INTRODUCTION

Over the past few years, much attention has been devoted to the effects of quantum interference between multiple atomic transitions pathways and its applications in quantum optics and laser physics. (A recent review has been presented by Arimondo [1].) One basic system consists of a V-type atom, with a single ground state and a closely spaced excited doublet, damped by the usual vacuum interactions, so that the two decay pathways from the excited doublet to the ground state are not independent. As the atom decays from one of the excited doublets it drives the other excited sublevel and vice versa. One well-known effect of radiative interference in such an atomic system is quantum beat oscillations of the fluorescence intensity [2–4], which has been observed in many laboratories [5]. Recent studies have also shown that radiative interference results in periodic dark states when the atom is initially in a coherent superposition state of the excited doublet [4], and a dark spectral line in the steady-state spontaneous emission spectrum [3]. This dark state is attributed to an interference-induced trapped state [6]. We have examined recently the probe absorption spectrum [7] and demonstrated that quantum interference in such a system is also the origin of narrow resonances, transparency, and gain without population inversion.

By introducing an applied field, Cardimona, Raymer, and Stroud [8] studied the effect of quantum interference on resonance fluorescence and found that the system can be driven into a dark state in which quantum interference prevents any fluorescence from the excited sublevels, regardless of the intensity of the excited laser. Similar predictions were reported by Scully *et al.* [9], who showed that if the two upper levels of a V-type quantum beat laser are coupled by a microwave field, an atom in the ground state may absorb pump photons and at the same time be free of radiative decay, even if population inversion occurs. The macroscopic dark periods of fluorescence emissions due to quantum interference in such a system have been demonstrated by Hegerfeldt and Plenio [10], using quantum jump theory. We have shown recently that the quantum interference can also give rise to a very narrow resonance [11], with linewidth depending on the splitting of the excited doublet as well as the Rabi frequency of the driving field.

Harris and co-workers [12] generalized the V-type atom to systems where the excited doublet decays to a continuum or to a single auxiliary level, in addition to the ground state. They found that at a certain frequency the absorption rate goes to zero due to destructive interference, whereas the emission rate remains finite. It is possible to amplify a laser field at this frequency without population inversion being present. In the case of a single auxiliary level, quantum interference can lead to the elimination of the spectral line at the driving laser frequency in the spontaneous emission spectrum [13], which has been recently observed by Xia *et al.* [14] in sodium dimers with the dipole moments of the two upper levels for the spontaneous emission being parallel (or antiparallel). An appealing physical picture for the observed spontaneous emission cancellation has been developed very recently by Agarwal [15].

Generally, for three-level atomic systems (in V, Λ, and Ξ configurations) excited by two laser fields, one being a strong pump field to drive two levels (say $|1\rangle$ and $|2\rangle$) and the other being a weak probe field at different frequency to probe the levels $|0\rangle$ and $|1\rangle$ or $|2\rangle$, the strong coherent field can drive the levels $|1\rangle$ and $|2\rangle$ into superpositions of these states (dressed states). Hence the weak field actually probes the state $|0\rangle$ and two dressed states, and two correlated transition channels (from the level $|0\rangle$ to the dressed levels) are created for atomic absorption. Quantum interference between the laser-induced transition pathways can be constructive or destructive, depending on the energy of the state $|0\rangle$ [16,17]. If $|0\rangle$ is the ground state of the three-level atom, the interference is destructive; otherwise, it is constructive. The destructive interference can cancel the probe absorption from the ground state to the dressed state, and the spontaneous emission of the reverse process, thus resulting in probe transparency [18], optical amplification without population inversion [19], enhancement of the refractive index with zero absorp-

*Electronic address: peng@qo1.am.qub.ac.uk
†Electronic address: sswain@qub.ac.uk

tion [20], spectral line narrowing [21–23], as well as a dark line in spontaneous emission from one of the excited sublevels [16]. The experimental observation of the destructive interference between the transition probability amplitudes from the ground state to the excited doublets (dressed states) in electromagnetically induced transparency has been presented recently [24]. Laser oscillation without population inversion via quantum interference also has been demonstrated experimentally in several atomic systems [25]. Both theory and experiment agree very well.

Recently, Camparo and Lambropoulos [26] have demonstrated a phase-sensitive rate of atomic excitation due to quantum interference between a three-photon transition and a one-photon transition pathway. Quantum interference features in three-photon down-conversion in phase space also have been reported [27]. The modulation of the two-photon excitation rate of Ξ-type atoms, as a function of the relative phase of multiple excitation fields, has been observed by Georgiades *at al.* [28], which may be applied to a recently developed frequency metrological technique and to detection of nonclassical correlation functions of fields. We have shown that quantum interference between the stepwise two-photon transition pathway and the one-step two-photon transition pathway in the nonclassical two-photon excitation of atoms can lead to a very narrow spectral line in the fluorescence spectrum [29].

Narrow spectral features have been predicted previously for other, related systems. Indeed, such effects are a possibility in any system where very small decay rates exist, whatever their origin. Buzek [30] has shown the existence of very narrow lines in the spectrum emitted by a system of N two-level atoms in which only one atom is initially excited, when the separation between the atoms is very small but nonzero. The presence of extremely sharp structures in the fluorescence of a three-level V system with one metastable excited level has been demonstrated by Hegerfeld and Plenio for the resonance fluorescence spectrum and in absorption by Plenio [31] (see also [32]). These effects have been attributed to ''electron shelving,'' the existence of light and dark periods in the resonance fluorescence emitted on the strong transition. They have also shown that a Λ system driven by a single laser, having close-lying lower levels and parallel transition moments, may exhibit light and dark periods similar to those exhibited by the well-known Dehmelt V system [33]. The unitary equivalence between the V system with cross-decay terms and doubly driven three-level systems with two closely spaced levels coupled by an intense microwave field has been demonstrated [34,31]. There are thus several distinct physical phenomena that will produce effects equivalent to those described, and the experimenter may choose the most appropriate. Narducci *et al.* [22] also considered a V-type atomic system in which two excited levels are coupled to the ground state by different laser fields, with one strongly driven and one weakly driven transition. They found line narrowing to be possible on the strong transition.

In this paper we consider a V-type atom consisting of two excited sublevels coupled to a singlet ground level by a single-mode laser field as shown in Fig. 1. Here we examine the effect of quantum interference on the spectral features of the resonance fluorescence emissions. Our organization is as follows. In Sec. II we present the formulism and numerical results of the incoherent resonance fluorescence spectrum. We find that an additional sharp peak arises at line center over wide ranges of the parameters if the effect of radiative interference is taken into account. When the applied field is tuned to a special frequency the fluorescent emission can be completely quenched in the presence of maximum quantum interference. We also demonstrate that the latter corresponds to the atom being in a pure state. A physical understanding of these results is obtained by invoking the dressed atom approach in Sec. III. According to this theory, the width of the central sharp line is proportional to the square of the excited doublet splitting. Thus extremely sharp lines, less than 1% of the natural linewidth, are possible. We investigate the effect of laser linewidth on the interference-induced phenomena in Sec. IV. The conclusions are summarized in Sec. V.

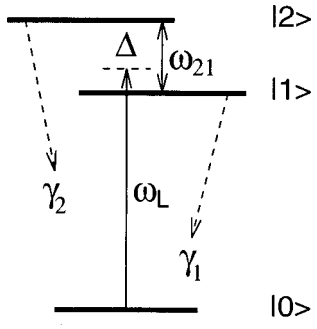

FIG. 1. A V atom driven by a single-mode laser.

II. RESONANCE FLUORESCENCE SPECTRUM

We consider a V-type atom consisting of two excited sublevels $|1\rangle$ and $|2\rangle$ coupled to a common ground level $|0\rangle$ by a single-mode laser field with amplitude E_L and phase ϕ_L. The energy-level scheme is shown in Fig. 1. The Hamiltonian in the frame rotating with the laser frequency ω_L is of the form

$$H=(\Delta-\omega_{21})A_{11}+\Delta A_{22}+[(\Omega_1 A_{10}+\Omega_2 A_{20})e^{-i\phi_L}+\text{H.c.}], \tag{1}$$

where $\Delta=(E_2-E_0)-\omega_L$ is the detuning between the $|0\rangle\leftrightarrow|2\rangle$ transition and the driving laser, $\Omega_k=E_L\mathbf{e}_L\cdot\mathbf{d}_{k0}$ $(k=1,2)$ is the Rabi frequency, $\mathbf{d}_{k0}$ is the dipole moment of the atomic transition from $|0\rangle$ to $|k\rangle$, which is assumed to be real in our system, and $\omega_{21}=E_2-E_1$ is the level splitting between the excited sublevels $|1\rangle$ and $|2\rangle$. $A_{lk}=|l\rangle\langle k|$ represents a population operator for $l=k$ and a dipole transition operator for $l\neq k$. Here direct transitions between the excited sublevels $|1\rangle$ and $|2\rangle$ are dipole forbidden. We use units such that $\hbar=1$.

Assuming that such an atomic system is damped by the standard vacuum, the master equation for the reduced density operator ρ of the atom in the rotating frame then takes the form [6–8,11,35]

$$\dot{\rho}=-i[H,\rho]+\frac{1}{2}\gamma_1(2A_{01}\rho A_{10}-A_{11}\rho-\rho A_{11})+\frac{1}{2}\gamma_2(2A_{02}\rho A_{20}-A_{22}\rho-\rho A_{22})+\frac{1}{2}\gamma_{12}(2A_{01}\rho A_{20}-A_{21}\rho-\rho A_{21})+\frac{1}{2}\gamma_{12}(2A_{02}\rho A_{10}-A_{12}\rho-\rho A_{12}), \quad (2)$$

where γ_k is the spontaneous decay constant of the excited sublevel $k(k=1,2)$ to the ground level $|0\rangle$. However, γ_{12} represents the effect of quantum interference resulting from the cross coupling between the transitions $|1\rangle\leftrightarrow|0\rangle$ and $|2\rangle\leftrightarrow|0\rangle$. It reflects the fact that as the atom decays from the excited sublevel $|1\rangle$ it drives the other excited sublevel $|2\rangle$ and vice versa. The effects of quantum interference are very sensitive to the orientations of the atomic dipole polarizations. If $\mathbf{d}_{10}$ is parallel to $\mathbf{d}_{20}$, then $\gamma_{12}=\sqrt{\gamma_1\gamma_2}$ and the interference effect is maximum, while if $\mathbf{d}_{10}$ is perpendicular to $\mathbf{d}_{20}$, then $\gamma_{12}=0$ and the quantum interference disappears. The quantity γ_{12} plays a crucial important role in the spectral narrowing and fluorescence quenching of the system considered here. The equations of motion of the reduced density matrix elements for the atomic variables take the form [8,11]

$$\dot{\rho}_{10}=-\left[\frac{1}{2}\gamma_1+i(\Delta-\omega_{21})\right]\rho_{10}-\frac{1}{2}\gamma_{12}\rho_{20}+i\Omega_2\rho_{12}+i\Omega_1(\rho_{11}-\rho_{00}), \quad (3a)$$

$$\dot{\rho}_{20}=-\left(\frac{1}{2}\gamma_2+i\Delta\right)\rho_{20}-\frac{1}{2}\gamma_{12}\rho_{10}+i\Omega_1\rho_{21}+i\Omega_2(\rho_{22}-\rho_{00}), \quad (3b)$$

$$\dot{\rho}_{21}=-\left[\frac{1}{2}(\gamma_1+\gamma_2)+i\omega_{21}\right]\rho_{21}-\frac{1}{2}\gamma_{12}(\rho_{22}+\rho_{11})+i\Omega_1\rho_{20}-i\Omega_2\rho_{01}, \quad (3c)$$

$$\dot{\rho}_{11}=-\gamma_1\rho_{11}-\frac{1}{2}\gamma_{12}(\rho_{12}+\rho_{21})-i\Omega_1(\rho_{01}-\rho_{10}), \quad (3d)$$

$$\dot{\rho}_{22}=-\gamma_2\rho_{22}-\frac{1}{2}\gamma_{12}(\rho_{12}+\rho_{21})-i\Omega_2(\rho_{02}-\rho_{20}). \quad (3e)$$

The fluorescence emission spectrum is proportional to the Fourier transformation of the steady-state correlation function $\lim_{t\to\infty}\langle\mathbf{E}^{(-)}(\mathbf{r},\tau+t)\cdot\mathbf{E}^{(+)}(\mathbf{r},t)\rangle$ [36], where $\mathbf{E}^{(\pm)}(\mathbf{r},t)$ are the positive and negative frequency parts of the radiation field in the far zone, which consists of a free-field operator and a source-field that is proportional to the atomic polarization operator. Therefore, the fluorescence spectrum can be expressed in terms of the atomic correlation function

$$G(\omega)=\Re\int_0^\infty\lim_{t\to\infty}\langle\mathbf{D}^\dagger(\tau+t)\cdot\mathbf{D}(t)\rangle e^{-i\omega\tau}d\tau, \quad (4)$$

where $\mathbf{D}^\dagger(t)$ is the atomic polarization operator

$$\mathbf{D}^\dagger(t)=\mathbf{d}_{10}A_{10}(t)+\mathbf{d}_{20}A_{20}(t) \quad (5)$$

and $\Re$ denotes ''the real part.''

The fluorescence emission spectrum $G(\omega)$ is composed of coherent and incoherent components. The coherent Rayleigh part, whose origin can be traced to the elastic scattering of the driving field, gives rise to only δ-function contributions, while the incoherent part stems from the fluctuations of the dipole polarizations. Hereafter we pay attention only to the incoherent resonance fluorescence spectrum, which is defined as

$$\Lambda(\omega)=\Re\int_0^\infty\lim_{t\to\infty}\langle\Delta\mathbf{D}^\dagger(\tau+t)\cdot\Delta\mathbf{D}(t)\rangle e^{-i\omega\tau}d\tau, \quad (6)$$

where $\Delta\mathbf{D}(\tau)=\mathbf{D}(\tau)-\langle\mathbf{D}(\infty)\rangle$ represents the deviation of the dipole polarization operator $\mathbf{D}(\tau)$ from its mean steady-state value. The two-time correlation function $\lim_{t\to\infty}\langle\Delta\mathbf{D}^\dagger(\tau+t)\cdot\Delta\mathbf{D}(t)\rangle$ can be obtained by invoking the quantum regression theorem [37], together with the equations (3a)–(3e) of motion. To do this, we define vectors $\mathbf{U}_j(t)$ $(j=1,2)$ for the steady-state two-time correlations of the atom

$$\mathbf{U}_j(t)=[\langle\Delta A_{20}(t)\Delta A_{0j}(0)\rangle,\ \langle\Delta A_{02}(t)\Delta A_{0j}(0)\rangle,\ \langle\Delta A_{22}(t)\Delta A_{0j}(0)\rangle,\ \langle\Delta A_{10}(t)\Delta A_{0j}(0)\rangle,\ \langle\Delta A_{01}(t)\Delta A_{0j}(0)\rangle,\ \langle\Delta A_{11}(t)\Delta A_{0j}(0)\rangle,\ \langle\Delta A_{21}(t)\Delta A_{0j}(0)\rangle,\ \langle\Delta A_{12}(t)\Delta A_{0j}(0)\rangle]^T. \quad (7)$$

According to the quantum regression theorem [37], when $t>0$ we have

$$\frac{d}{dt}\mathbf{U}_j(t)=\underline{\mathcal{M}}\mathbf{U}_j(t)\quad(j=1,2), \quad (8)$$

where $\underline{\mathcal{M}}$ is an 8×8 matrix of coefficients of the equations (3a)–(3e) of motion of the Bloch vector $\mathbf{B}(t)=[\langle A_{20}(t)\rangle,\langle A_{02}(t)\rangle,\langle A_{22}(t)\rangle,\langle A_{10}(t)\rangle,\langle A_{01}(t)\rangle,\langle A_{11}(t)\rangle,\langle A_{21}(t)\rangle,\langle A_{12}(t)\rangle]^T$. Note that $\langle A_{lk}(t)\rangle=\rho_{kl}(t)$. Due to the time independence of $\underline{\mathcal{M}}$, Eq. (8) is readily solved. Hence one obtains the incoherent resonance fluorescence spectrum to be

$$\Lambda(\omega)=\Re\sum_{k=1}^{8}\{R_{1k}(i\omega)[\gamma_2U_2^{(k)}(0)+\gamma_{12}U_1^{(k)}(0)]+R_{4k}(i\omega)[\gamma_1U_1^{(k)}(0)+\gamma_{12}U_2^{(k)}(0)]\}, \quad (9)$$

where $U_j^{(k)}(0)$ is the initial component of the vector $\mathbf{U}_j(t)$ $(j=1,2)$, defined in Eq. (7). $R_{jk}(i\omega)$ is one element of the matrix $\underline{\mathcal{R}}(i\omega)=(i\omega\underline{I}-\underline{\mathcal{M}})^{-1}$, with $\underline{I}$ being the identity matrix.

Defining $\alpha=d_{10}/d_{20}$ as the ratio of the dipole moment amplitudes of the two allowed transition pathways, we have the relationships $\gamma_1=\alpha^2\gamma_2=\alpha^2\gamma$ and $\Omega_1=\alpha\Omega_2=\alpha\Omega$. In what follows we take $\alpha=1$.

We first consider the case of the V atom with a degenerate excited doublet $\omega_{21}=0$, which actually serves as a two-level atom. The resonance fluorescence spectrum, as expected, consists of a single peak at line center for weak driving intensities (it is not displayed here) and a Mollow-like triplet for strong driving intensities. See, for example, in Fig. 2 for

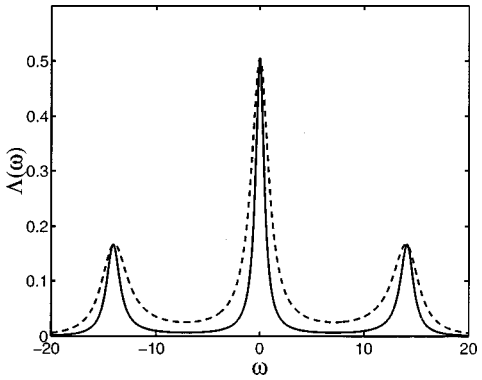

FIG. 2. The 2D incoherent resonance fluorescence spectrum $\Lambda(\omega)$ of the V atom with a degenerate excited doublet ($\omega_{21}=0$), as a function of ω, with $\Omega=5$, $\Delta=0$, and $\gamma_{12}=0$ (solid curve), or $\gamma_{12}=1$ (dashed curve), respectively. (All variables are scaled by γ throughout these figures where we take $\gamma=1$, for simplicity.)

$\Omega=5\gamma$ and $\Delta=0$, in which the solid and dashed curves are, respectively, for zero ($\gamma_{12}=0$) and maximum ($\gamma_{12}=\gamma$) degrees of quantum interference. As one sees, quantum interference broadens the Mollow-like triplet.

For the nondegenerate case, we display the resonance fluorescence spectrum for $\Delta=0$, $\Omega=5\gamma$, with various splittings of the excited doublet and different degrees of quantum interference in Fig. 3. One finds that for the given Rabi frequency $\Omega=5\gamma$, the spectrum exhibits a three-peak structure for a small splitting $\omega_{21}=\gamma$, shown in Figs. 3(a)–3(c), while the remaining spectrum consists of seven peaks for $\omega_{21}=5\gamma$. However, the most significant feature in the figure is a very narrow peak imposed on the central peak when the quantum interference between the two transition channels of the ground state to the excited doublet is taken into account. See, for instance, Figs. 3(b), 3(c), 3(e), and 3(f). The smaller the ratio of the level splitting to the Rabi frequency, the more pronounced the narrow spectral profile.

We next consider a special circumstance, $\Delta=\omega_{21}/2$ in Fig. 4, which shows once again that the incoherent fluorescence spectrum is dramatically modified by quantum interference. When the atom has nearly parallel dipole moments, for example, $\gamma_{12}=0.999\gamma$ in Figs. 4(b) and 4(e), a significant sharp peak occurs at line center. However, when the atomic transition dipole moments are exact parallel, i.e., $\gamma_{12}=\gamma$, the fluorescence emission quenches completely at all frequencies, as one sees in Figs. 4(c) and 4(f). The latter effect recently has been confirmed experimentally in a slightly different atomic system with parallel transition dipole moments under the condition $\Delta=\omega_{21}/2$ [14].

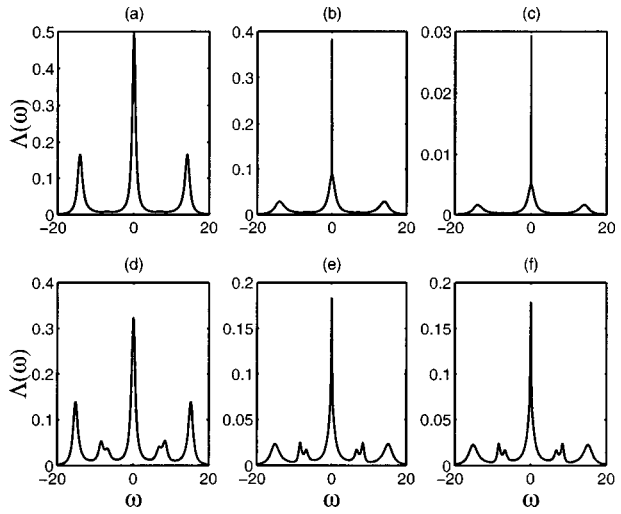

FIG. 3. Same as Fig. 2, but with a nondegenerate excited doublet ($\omega_{21}\neq 0$), for $\Omega=5$, $\Delta=0$, and (a) $\omega_{21}=1$, $\gamma_{12}=0$; (b) $\omega_{21}=1$, $\gamma_{12}=0.999$; (c) $\omega_{21}=1$, $\gamma_{12}=1$; (d) $\omega_{21}=5$, $\gamma_{12}=0$; (e) $\omega_{21}=5$, $\gamma_{12}=0.999$; and (f) $\omega_{21}=5$, $\gamma_{12}=1$.

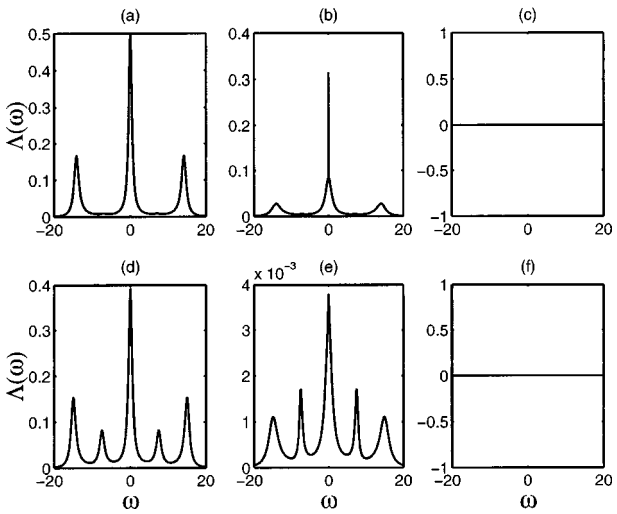

FIG. 4. Same as Fig. 3, but with $\Delta=\omega_{21}/2$.

We show three-dimensional plots of the central region of the spectrum in Figs. 5–8, in which the spectral narrowing occurs over very wide ranges of the parameters, not just the ones chosen in Figs. 3 and 4. See, for example, Fig. 5, where the detuning $\Delta=\omega_{21}/2$ and both dipole transition monents are nearly parallel $\gamma_{12}=0.999\gamma$. The splitting ω_{21} has the values $\omega_{21}=\gamma$ in Fig. 5(a) and $\omega_{21}=5\gamma$ in Fig. 5(b). These figures clearly show that the larger the Rabi frequency, the narrower the interference-induced peak, and the smaller the splittings of the excited sublevels (for fixed Rabi frequency), the more pronounced the narrow spectrum. This conclusion also fits with other cases, for instance, in Fig. 6, where the splitting is large $\omega_{21}=20\gamma$ and the detuning $\Delta=0$ [Fig. 6(a)] and $\Delta=50\gamma$ [Fig. 6(b)]. These graphs clearly exhibit how the spectral narrowing develops as the Rabi frequency increases.

Figure 7 displays the three-dimensional (3D) spectrum in the case of $\Omega=50\gamma$, $\Delta=30\gamma$, and $\gamma_{12}=0.999\gamma$, against the splitting of the excited sublevels ω_{21}/γ. Apparently, the narrowest spectral line occurs at $\omega_{21}\sim 3\gamma$. The linewidth is approximately $\gamma/300$. As the splitting increases, the central spectrum broadens.

We present the 3D resonance fluorescence spectrum as a function of the detuning Δ/γ in Fig. 8, for $\gamma_{12}=\gamma$ and (a) $\Omega=5\gamma$, $\omega_{21}=\gamma$ and (b) $\Omega=100\gamma$, $\omega_{21}=40\gamma$, from which one can see that the most significant line narrowing occurs around $\Delta=-4.5\gamma$ and 5.5γ in Fig. 8(a) and $\Delta=-80\gamma$ and 120γ in Fig. 8(b). The fluorescence quenching occurs at $\Delta=0.5\gamma$ and $\Delta=20\gamma$, respectively.

We examine the atomic purity in Fig. 9 for $\Omega=5\gamma$ and $\omega_{21}=10\gamma$ as a function of γ_{12} and Δ. The purity $\mathcal{P}$ is defined as [35]

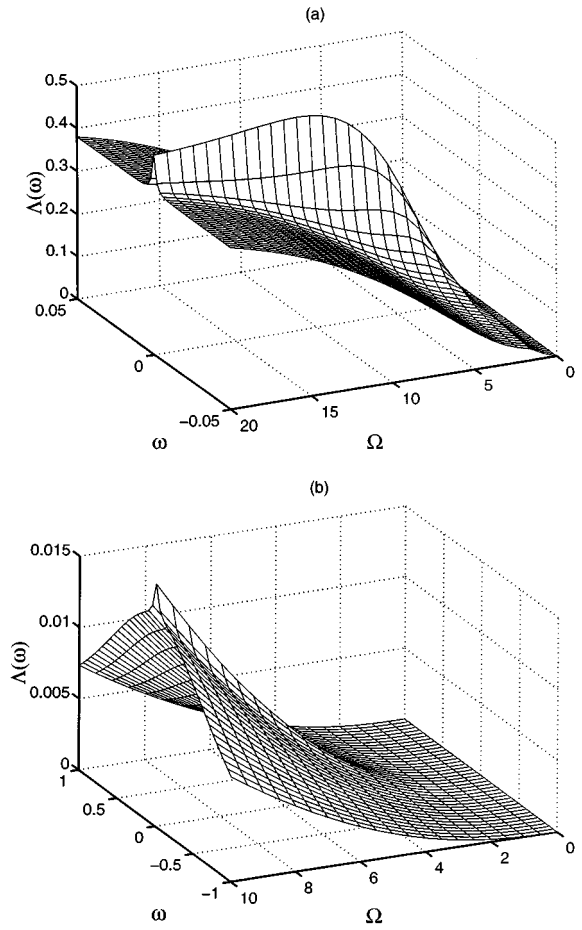

FIG. 5. The 3D spectrum versus ω and Ω, for $\gamma_{12}=0.999$, $\Delta=\omega_{21}/2$, and (a) $\omega_{21}=1$ and (b) $\omega_{21}=5$.

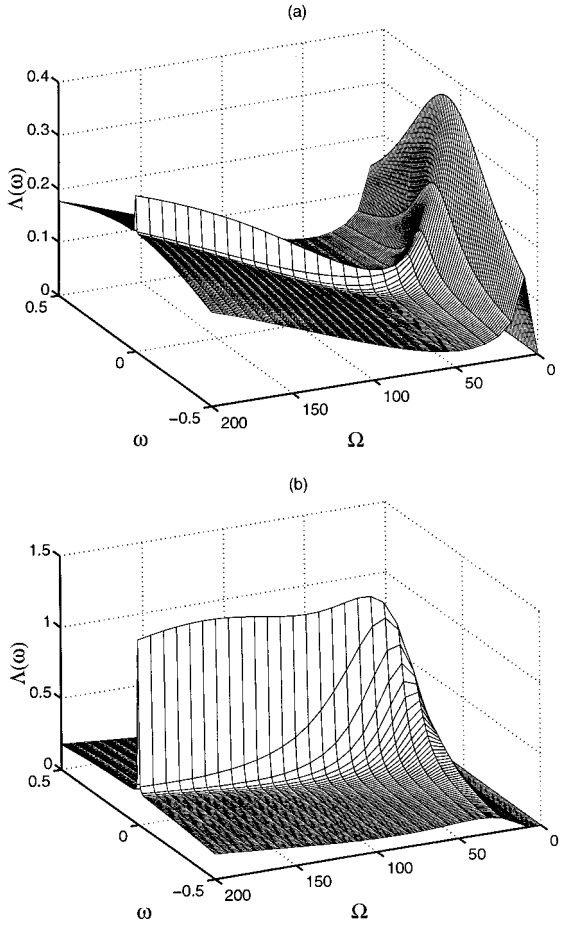

FIG. 6. Same as Fig. 5, but for $\gamma_{12}=0.999$, $\omega_{21}=20$, and (a) $\Delta=0$ and (b) $\Delta=50$.

$$\mathcal{P}=\mathrm{Tr}(\rho^2)=\rho_{00}^2+\rho_{11}^2+\rho_{22}^2+2(|\rho_{10}|^2+|\rho_{20}|^2+|\rho_{21}|^2). \tag{10}$$

$\mathcal{P}=1$ corresponds to a pure state of the atom, while $\mathcal{P}=1/3$ represents the maximum mixed state of the atom, an unpolarized state. Obviously, one sees from Fig. 9 that the atomic purity in the vicinity of $\Delta=\omega_{21}/2$ is strongly dependent on the quantum interference. An atomic pure state can be achieved at $\Delta=\omega_{21}/2$ with the maximum quantum interference, whereas for $\gamma_{12}\simeq 0$, we have a maximally mixed state. We shall see in the following section that the pure state involved is a dressed state. This implies that the atomic energy is completely trapped in the pure state, which prevents any photon from emitting, giving rise to fluorescence quenching.

III. ORIGIN OF SPECTRAL NARROWING AND FLUORESCENCE QUENCHING

To explore the origins of the unusual spectral features produced by quantum interference we employ the dressed-atomic-state representation [38], which makes the physical processes transparent, to derive a compact form of the resonance fluorescence spectrum. For simplicity, we here assume that the excitation field is tuned to

$$\Delta=\omega_{21}/2 \tag{11}$$

and the magnitudes of both dipole moments to be identical (so that $\gamma_1=\gamma_2=\gamma$ and $\Omega_1=\Omega_2=\Omega$). In this situation, the eigenvalues and eigenstates of the interaction Hamiltonian (1) are given by

$$\lambda_a=-\frac{1}{2}\Omega_R, \quad \lambda_b=0, \quad \lambda_c=\frac{1}{2}\Omega_R \tag{12}$$

and

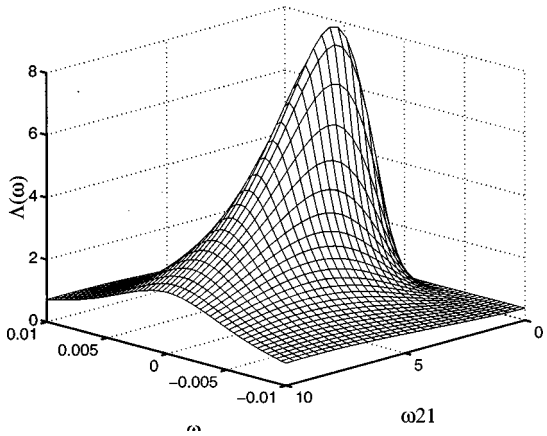

FIG. 7. The 3D spectrum against ω and ω_{21}, for $\gamma_{12}=0.999$, $\Omega=50$, and $\Delta=30$.

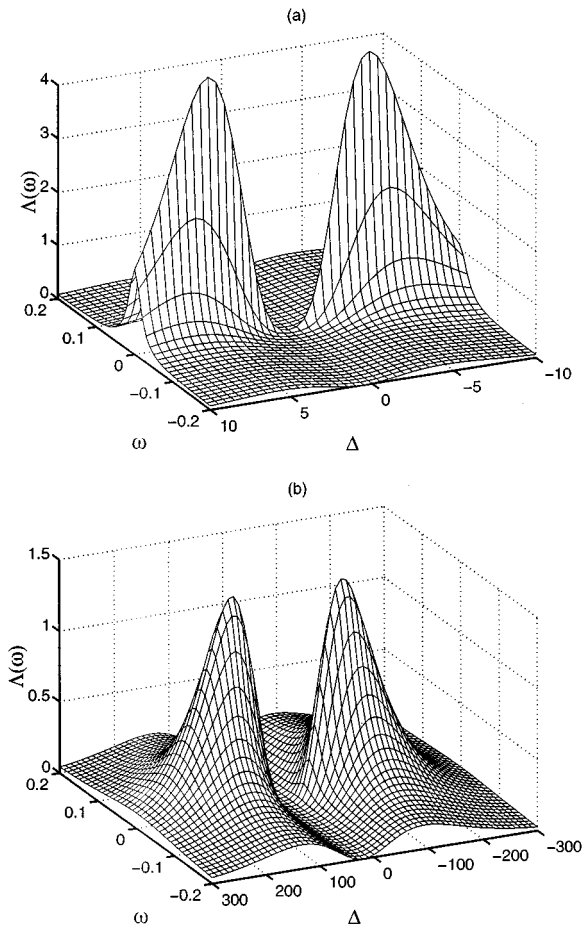

FIG. 8. The 3D spectrum against ω and Δ, for $\gamma_{12}=1$ and (a) $\Omega=5$, $\omega_{21}=1$ and (b) $\Omega=100$, $\omega_{21}=40$.

$$|a\rangle=\frac{1}{2}[-(1-\varepsilon)|2\rangle-(1+\varepsilon)|1\rangle+4\eta|0\rangle],$$

$$|b\rangle=-2\eta|2\rangle+2\eta|1\rangle+\varepsilon|0\rangle,$$

$$|c\rangle=\frac{1}{2}[(1+\varepsilon)|2\rangle+(1-\varepsilon)|1\rangle+4\eta|0\rangle], \tag{13}$$

where

$$\Omega_R=\sqrt{\omega_{21}^2+8\Omega^2},\quad \eta=\frac{\Omega}{\Omega_R},\quad \varepsilon=\frac{\omega_{21}}{\Omega_R}. \tag{14}$$

In the high-field limit, where the effective Rabi frequency is much greater than all relaxation rates, i.e., $\Omega_R\gg\gamma$, the coupling between matrix elements associated with various frequencies may be omitted to $O(\gamma/\Omega_R)$. Correspondingly, the equations of motion in the dressed-state representation are obtained as

$$\dot{\rho}_{bb}\simeq-\Gamma_1\rho_{bb}+\Gamma_0,$$

$$\dot{\rho}_{cc}-\dot{\rho}_{aa}\simeq-\Gamma_2(\rho_{cc}-\rho_{aa}),$$

$$\dot{\rho}_{ab}\simeq-\left(\Gamma_3-i\frac{1}{2}\Omega_R\right)\rho_{ab}+\Gamma_4\rho_{bc},$$

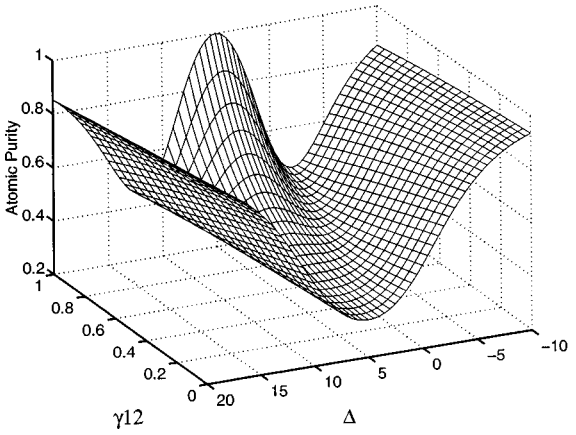

FIG. 9. The 3D atomic purity versus γ_{12} and Δ, for $\omega_{21}=10$ and $\Omega=5$.

$$\dot{\rho}_{cb}\simeq-\left(\Gamma_3+i\frac{1}{2}\Omega_R\right)\rho_{cb}+\Gamma_4\rho_{ba},$$

$$\dot{\rho}_{ac}\simeq-(\Gamma_5-i\Omega_R)\rho_{ac}, \tag{15}$$

with

$$\Gamma_0=\frac{1}{2}[(\gamma+\gamma_{12})\varepsilon^2+(\gamma-\gamma_{12})\varepsilon^4],$$

$$\Gamma_1=\frac{1}{2}[(\gamma+\gamma_{12})\varepsilon^2+(\gamma-\gamma_{12})(3\varepsilon^4-4\varepsilon^2+2)],$$

$$\Gamma_2=\frac{1}{2}[(\gamma+\gamma_{12})+(\gamma-\gamma_{12})\varepsilon^2],$$

$$\Gamma_3=\frac{1}{4}[2\gamma+(\gamma-\gamma_{12})(1+\varepsilon^2-2\varepsilon^4)],$$

$$\Gamma_4=-\frac{1}{2}(\gamma-\gamma_{12})(1-\varepsilon^2)\varepsilon^2,$$

$$\Gamma_5=\frac{1}{4}[3(\gamma+\gamma_{12})+(\gamma-\gamma_{12})\varepsilon^4-\gamma_{12}2\varepsilon^2]. \tag{16}$$

Only the diagonal elements are nonzero in the steady state:

$$\rho_{aa}=\rho_{cc}=\frac{\Gamma_1-\Gamma_0}{2\Gamma_1},\quad \rho_{bb}=\frac{\Gamma_0}{\Gamma_1}. \tag{17}$$

It is not difficult to see, in the presence of maximum quantum interference $\gamma_{12}=\gamma$, that $\rho_{aa}=\rho_{cc}=0$ and $\rho_{bb}=1$: the atom is trapped in the dressed state $|b\rangle$. Therefore, there is no fluorescence at all in this circumstance.

Under the secular approximation, the incoherent resonance fluorescence spectrum can be expressed as an analytical form

$$\Lambda(\omega)=\frac{1}{4}\Re\left[\frac{A_1}{\Gamma_1+i\omega}+\frac{A_2}{\Gamma_2+i\omega}+\frac{A_3}{\Gamma_3-\Gamma_4+i(\omega+\Omega_R/2)}+\frac{A_4}{\Gamma_3+\Gamma_4+i(\omega+\Omega_R/2)}+\frac{A_5}{\Gamma_3-\Gamma_4+i(\omega-\Omega_R/2)}+\frac{A_6}{\Gamma_3+\Gamma_4+i(\omega-\Omega_R/2)}+\frac{A_7}{\Gamma_5+i(\omega+\Omega_R)}+\frac{A_8}{\Gamma_5+i(\omega-\Omega_R)}\right], \tag{18}$$

where

$$A_1=9(\gamma-\gamma_{12})\varepsilon^2(1-\varepsilon^2)(\rho_{aa}+\rho_{cc})\rho_{bb},$$

$$A_2=(\gamma+\gamma_{12})(1-\varepsilon^2)[(\rho_{aa}+\rho_{cc})\rho_{bb}+4\rho_{aa}\rho_{cc}],$$

$$A_3=(\gamma-\gamma_{12})[(1-\varepsilon^2)(1-2\varepsilon^2)\rho_{bb}+2\varepsilon^4\rho_{aa}]+2\gamma_{12}\varepsilon^2\rho_{aa},$$

$$A_4=(\gamma-\gamma_{12})(1-\varepsilon^2)\rho_{bb}+2\gamma\varepsilon^2\rho_{aa},$$

$$A_5=(\gamma-\gamma_{12})[(1-\varepsilon^2)(1-2\varepsilon^2)\rho_{bb}+2\varepsilon^4\rho_{cc}]+2\gamma_{12}\varepsilon^2\rho_{cc},$$

$$A_6=(\gamma-\gamma_{12})(1-\varepsilon^2)\rho_{bb}+2\gamma\varepsilon^2\rho_{cc},$$

$$A_7=[\gamma+\gamma_{12}+(\gamma-\gamma_{12})\varepsilon^2](1-\varepsilon^2)\rho_{aa},$$

$$A_8=[\gamma+\gamma_{12}+(\gamma-\gamma_{12})\varepsilon^2](1-\varepsilon^2)\rho_{cc}. \tag{19}$$

The incoherent resonance fluorescence spectrum for the detuning (11) consists of five spectral components: the central resonance, the inner sidebands placed at frequencies $\pm\Omega_R/2$, and the outer sidebands located at frequencies $\pm\Omega_R$.

In the dressed-state representation, the underlying physical processes are evident. Various components are associated with different transitions in the dressed states. The central peak comes from transitions between the same level of two neighboring manifolds of the dressed states and consists of a superposition of two Lorentzians with linewidths $2\Gamma_1$ and $2\Gamma_2$, which are related to the decay rates of the population ρ_{bb} in the dressed state $|b\rangle$ and of the population difference $\rho_{cc}-\rho_{aa}$ of the dressed states $|a\rangle$ and $|c\rangle$, respectively. However, one (located at $-\Omega_R/2$) of the inner sidebands is the result of the transitions from $|a\rangle$ to $|b\rangle$ and from $|b\rangle$ to $|c\rangle$. Both transitions couple each other, so the spectral line is a superposition of two Lorentzians with linewidths $2(\Gamma_3\pm\Gamma_4)$, which are associated with the decays of the dressed-state coherences $\rho_{ab}\pm\rho_{bc}$. The other inner sideband is associated with the transitions $|c\rangle\rightarrow|b\rangle$ and $|b\rangle\rightarrow|a\rangle$. This peak is also composed of two Lorentzians with linewidths $2(\Gamma_3\pm\Gamma_4)$, but they are the results of the decays of the dressed-state coherences $\rho_{cb}\pm\rho_{ba}$. Transitions between the dressed states $|a\rangle$ and $|c\rangle$ contribute the outer sidebands. Since the stationary dressed-state populations ρ_{aa} and ρ_{cc} are identical in the secular approximation, the spectrum is symmetric.

A. The case of the degenerate excited sublevels: $\omega_{21}=0$

For the V atom with two degenerate excited sublevels, the steady-state populations of the dressed state reduce to $\rho_{aa}=\rho_{cc}=1/2$, $\rho_{bb}=0$, which demonstrates that the atom stays only in the dressed states $|b\rangle$ and $|c\rangle$. The transition amplitudes associated with the dressed state $|b\rangle$ thus are zero. The resultant spectrum gives a triplet structure of the form

$$\Lambda(\omega)=\frac{(\gamma+\gamma_{12})^2}{8}\left\{\frac{1}{\frac{1}{4}(\gamma+\gamma_{12})^2+\omega^2}+\frac{3/4}{\frac{9}{16}(\gamma+\gamma_{12})^2+(\omega+\sqrt{8}\Omega)^2}+\frac{3/4}{\frac{9}{16}(\gamma+\gamma_{12})^2+(\omega-\sqrt{8}\Omega)^2}\right\}, \tag{20}$$

which resembles the Mollow spectrum of a two-level atom. It is not difficult to see that the ratios of the height and width of the central peaks to those of the sidebands are 3 and 2/3, respectively, the same as in the Mollow triplet [39]. However, the sidebands are displaced by $\sqrt{8}\Omega$ from line center, instead of Ω as in the original Mollow case. In addition, the widths of the central and sideband peaks, $(\gamma+\gamma_{12})$ and $3(\gamma+\gamma_{12})/2$, respectively, which also differ from the Mollow values, γ and $3\gamma/2$, are sensitive to the degree of quantum interference. Quantum interference always broadens the spectral lines in the case of $\omega_{21}=0$.

B. The case of the nondegenerate excited sublevels: $\omega_{21}\neq 0$

In Sec. II we found that quantum interference can result in spectral line narrowing and fluorescence quenching when the excited doublet is nondegenerate. The analytical expression (18) for the resonance fluorescence spectrum allows greater insight into the physical mechanisms of these interference-induced effects.

1. Fluorescence quenching

It is apparent from Eq. (17) that if $\gamma_{12}=\gamma$, i.e., the dipole moments of the two transitions are exactly parallel, then $\rho_{aa}=\rho_{aa}=0$ and $\rho_{bb}=1$, and the population is entirely trapped in the dressed state $|b\rangle$. Consequently, $A_j=0$, $(j=1,2,\ldots,8)$ in Eq. (18), which implies $\Lambda(\omega)=0$, no fluorescence at all. Fluorescence quenching is due to completely destructive interference.

However, if γ_{12} deviates from the maximum value γ, which makes the destructive quantum interference incomplete, then $\rho_{aa}=\rho_{cc}\neq 0$ and fluorescent emission becomes possible. On the other hand, it is apparent that the amplitudes of the fluorescence spectrum (18) are maximal in the absence of quantum interference $(\gamma_{12}=0)$, the case in which the dipole moments are perpendicular.

It is worth emphasizing that the fluorescence quenching effect is not just restricted in the special case of $\alpha=1$. In

fact, as long as the dipole moments of the two transitions are exactly parallel $\gamma_{12}=\sqrt{\gamma_1\gamma_2}$ and the detuning satisfies that $\Delta=\omega_{21}/(1+\alpha^2)$, then the population is always trapped in the dressed state $|b\rangle$ and the fluorescence radiation will be suppressed completely, no matter what values of α, ω_{21}, and $\Omega_{1(2)}$ are taken.

2. Spectral narrowing

As we have shown above, an extremely narrow peak may arise at line center when the atomic dipole moments are nearly parallel. In order to explore the physical origin of the spectral narrowing employing the analytical results we assume that γ_{12} has a value slightly less than its maximum $\sqrt{\gamma_1\gamma_2}$. In this case, the dressed states $|a\rangle$ and $|c\rangle$ have a very small, but nonzero, population. As a consequence, some fluorescent emission may take place, $\Lambda(\omega)\neq 0$, and the linewidths of two Lorentzians forming the central component of the spectrum are reduced to $\Gamma_1\simeq\gamma\varepsilon^2$ and $\Gamma_2\simeq\gamma$, respectively. Hence, if $\varepsilon\ll 1$, which requires that the splitting ω_{21} of the excited sublevels be much less than the effective Rabi frequency Ω_R, then $\Gamma_1\ll\gamma$, a very narrow Lorentzian line shape. However, the other Lorentzian always has a linewidth of order γ. Thus the spectral feature at line center consists of a sharp peak superimposed on a broad Lorentzian profile. We emphasize that the sharp peak can be very narrow. For example, the linewidth in Fig. 4(b) is predicted to be $\Gamma_1\simeq\gamma/100$ by the dressed state theory and found to be so numerically. The linewidth of the sharp feature in Figs. 3(b) and 3(c) is also close to this value.

We conclude that the spectral narrowing is due to a slowly decay of the dressed-state population ρ_{bb}, which originates certainly from quantum interference between two transition pathways. In fact, when γ_{12} is far from the maximum allowed value γ, the decay rate of the population in the dressed state $|b\rangle$ increases and becomes comparable with Γ_2. In the case of $\gamma_{12}=0$, no quantum interference, $\Gamma_1=\gamma(3\varepsilon^4-3\varepsilon^2+2)/2$ and $\Gamma_2=\gamma(1+\varepsilon^2)/2$, leading to two Lorentzians with linewidths wider than γ, and no narrow spectral feature is exhibited.

In addition, quantum interference can also narrow the sidebands. See, for example, Figs. 4(d) and 4(e). The former is in absence of quantum interference ($\gamma_{12}=0$) and the linewidth of the inner sidebands is approximately 1.6γ, while in the latter figure the inner linewidth is γ when a nearly maximum value ($\gamma_{12}=0.999\gamma$) of quantum interference is taken. However, the linewidth of the outer sidebands increases from 1.5γ to 2.9γ when γ_{12} increases from 0 to 0.999γ in this case. The modifications are due to influence of the quantum interference on the decays of the dressed-state coherences.

We turn to the effect of the splitting of the excited sublevels on the spectral structure. One finds from formula (18) that when the splitting is very small, i.e., $\varepsilon\ll 1$, the heights of the central, inner, and outer sidebands are approximately proportional to $(\gamma^2-\gamma_{12}^2)(1-3\varepsilon^2)$, $(\gamma^2-\gamma_{12}^2)\varepsilon^2$, and $(\gamma-\gamma_{12})(1-2\varepsilon^2)$, respectively. Therefore, the inner sidebands are hardly visible in the case of $\varepsilon\sim 0$, as we see, for example, in Figs. 4(a) and 4(b), where the resonance fluorescence spectrum demonstrates a Mollow-like triplet. However, the inner sidebands become visible with increasing splitting, as shown in Figs. 4(d) and 4(e), with the inner sidebands even being more pronounced than the outer sidebands in the latter frame when quantum interference is taken into account.

In the general case, the dressed states $|a\rangle,|b\rangle,|c\rangle$ no longer have equally spaced splittings. As a result, the transitions of $|c\rangle\rightarrow|b\rangle$ and $|b\rangle\rightarrow|a\rangle$ will lead to two spectral lines and the spontaneous decays of $|a\rangle\rightarrow|b\rangle$ and $|b\rangle\rightarrow|c\rangle$ also give rise to different spectral components. Consequently, there exists a maximum of seven peaks, as may be seen in Figs. 3(d)–3(f), for example. In this circumstance, spectral narrowing at line center can still occur when $\varepsilon\ll 1$ and $\gamma_{12}\simeq\gamma$. See Figs. 3(e) and 3(f). This is also a result of the slow decay rate of one of the dressed state populations induced by the quantum interference.

We note that Narducci *et al.* [22] considered a V-type atomic system in which two excited levels are coupled to the ground state by different laser fields. When one transition is very weakly driven compared to the other, the spectral line arising from fluorescence from the strong transition can be narrowed. The spectral narrowing in such a system was later confirmed experimentally by Gauthier *et al.* [23]. Similar effects were also investigated, using the Green's-function method and quantum jump theory, respectively, by Fu *et al.* and Hegerfeldt and Plenio [40,31], who demonstrated that an additional sharp peak is superimposed at line center of the resonance fluorescence spectrum in the presence of a metastable excited state that is coupled the ground state by a very weak laser field and that the width of the narrow peak is essentially proportional to the intensity of the laser driving the metastable transition. The phenomenon can be classified into a kind of quantum jump proposed by Dehmelt [33].

IV. EFFECT OF LASER LINEWIDTH

For more realistic cases, the driving laser may undergo various kinds of fluctuations, such as phase and amplitude diffusion, so that the laser output has a finite bandwidth. For operation above threshold the phase and amplitude fluctuations are decoupled and for a well-stabilized laser the amplitude fluctuations can be neglected. Therefore, we consider only a driving laser subject to the phase diffusion effect. The corresponding Hamiltonian (1) is replaced by

$$H=(\Delta-\omega_{21})A_{11}+\Delta A_{22}+[(\Omega_1A_{10}+\Omega_2A_{20})e^{-i\Phi(t)}+\text{H.c.}], \tag{21}$$

where $\Phi(t)=\phi_L+\phi(t)$ and $\phi(t)$ is the fluctuating part of the phase of the driving laser, which is assumed to be a Gaussian random process with the properties

$$\dot{\phi}(t)=F(t),\quad \langle F(t)\rangle=0,\quad \langle F(t)F(t')\rangle=2L\,\delta(t-t'), \tag{22}$$

where L is the linewidth of the driving laser due to the phase diffusion.

For such a laser model, the effect of the laser linewidths can be accounted for by modifying the equations (3a)–(3b) of motion for the off-diagonal elements of the density matrix as [41]

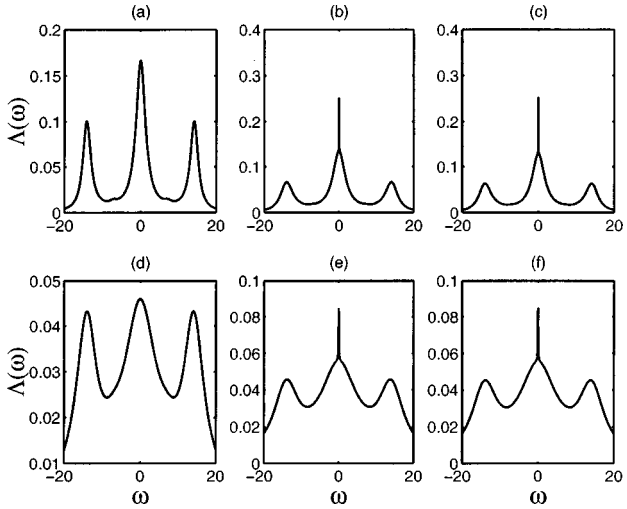

FIG. 10. The 2D resonance fluorescence spectrum including the effect of the laser linewidth, for $\Omega=5$, $\omega_{21}=1$, $\Delta=\omega_{21}/2$, and (a)–(c) $L=1$ and (d)–(f) $L=5$.

$$\dot{\rho}_{10}=-\left[\frac{1}{2}\gamma_1+L+i(\Delta-\omega_{21})\right]\rho_{10}-\frac{1}{2}\gamma_{12}\rho_{20}+i\Omega_2\rho_{12}+i\Omega_1(\rho_{11}-\rho_{00}), \tag{23a}$$

$$\dot{\rho}_{20}=-\left(\frac{1}{2}\gamma_2+L+i\Delta\right)\rho_{20}-\frac{1}{2}\gamma_{12}\rho_{10}+i\Omega_1\rho_{21}+i\Omega_2(\rho_{22}-\rho_{00}). \tag{23b}$$

The formulas preciously used to evaluate the spectrum are easily modified for this circumstance. We display the effect of laser linewidth in Fig. 10 for the case of $\Omega=5\gamma$, $\omega_{21}=\gamma$, $\Delta=\omega_{21}/2$, and $L=\gamma$ in Figs. 10(a)–10(c) and $L=5\gamma$ in Figs. 10(d)–10(f). It is clearly seen from Figs. 10(b), 10(c), 10(e), and 10(f) that the spectrum still exhibits a very sharp interference-induced peak imposed on the line center in the presence of laser linewidth. Comparing with Fig. 4, one finds that the laser linewidth has a twofold effect on the spectrum: first it broadens all spectral components (including the narrow spectral line) and reduces their heights and second it eliminates fluorescence quenching in the case $\gamma_{12}=\gamma$.

These effects may also be interpreted in the dressed representation. In the presence of nonzero laser linewidth the decay rates (16) of the dressed-state populations and coherences are modified by

$$\Gamma_0^L=\Gamma_0+L\varepsilon^2(1-\varepsilon^2),$$
$$\Gamma_1^L=\Gamma_1+3L\varepsilon^2(1-\varepsilon^2),$$
$$\Gamma_2^L=\Gamma_2+L(1-\varepsilon^2),$$
$$\Gamma_3^L=\Gamma_3+\frac{1}{2}L(1-\varepsilon^2+2\varepsilon^4),$$
$$\Gamma_4^L=\Gamma_4+L\varepsilon^2(1-\varepsilon^2),$$
$$\Gamma_5^L=\Gamma_5+\frac{1}{2}L(1-\varepsilon^4). \tag{24}$$

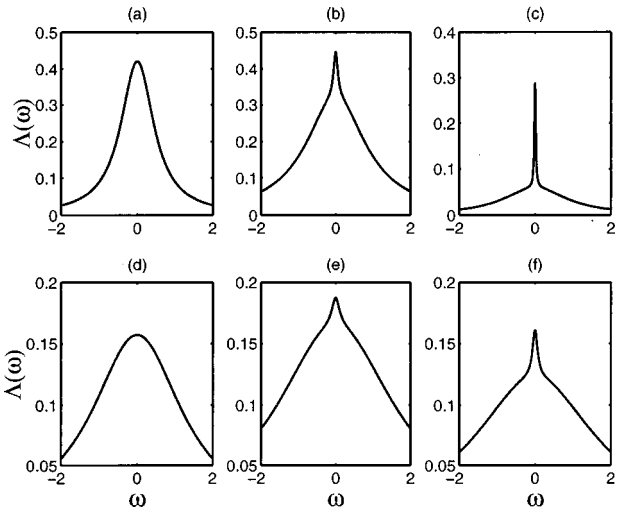

FIG. 11. Same as Fig. 10, but for $\omega_{21}=20$, $\Omega=50$, $\Delta=30$, and (a) $L=0$, $\gamma_{12}=0$; (b) $L=0$, $\gamma_{12}=0.99$; (c) $L=0$, $\gamma_{12}=1$; (d) $L=1$, $\gamma_{12}=0$; (e) $L=1$, $\gamma_{12}=0.99$; and (f) $L=1$, $\gamma_{12}=1$.

The corresponding steady-state populations and spectrum have the same forms as Eqs. (17) and (18), respectively, but with Γ_j being replaced by Γ_j^L $(j=0,1,\ldots,5)$. It is not difficult to show that the dressed-state populations in the case of the maximum quantum interference take the form

$$\rho_{aa}=\rho_{cc}=\frac{L(1-\varepsilon^2)}{\gamma+3L(1-\varepsilon^2)}, \quad \rho_{bb}=\frac{\gamma+L(1-\varepsilon^2)}{\gamma+3L(1-\varepsilon^2)}. \tag{25}$$

No population is trapped in a special state, so no fluorescence quenching occurs if the driving laser undergoes phase diffusion, and hence has a finite linewidth.

Although the presence of a laser linewidth always increases the dressed-state decay rates, broadens the spectral lines, and reduces their amplitudes, nevertheless, quantum interference can still lead to a very narrow spectral line. For example, in the case of $\varepsilon\ll 1$ and $\gamma_{21}\sim\gamma$, the linewidth of the sharp peak is approximately $2(\gamma+3L)\varepsilon^2$. As shown in Fig. 10, the linewidth of the narrow spectral line is about $\gamma/25$ in Figs. 10(b) and 10(c), whereas it approximates to $4\gamma/25$ in Figs. 10(e) and 10(f).

Figure 11 shows the central region of the spectrum including the effect of laser linewidth, for a large level splitting, strong Rabi frequency, and large detuning, say, $\omega_{21}=20\gamma$, $\Omega=50\gamma$, and $\Delta=30\gamma$. We take $L=0$ in Figs. 11(a)–11(c), whereas $L=\gamma$ in Figs. 11(d)–11(f). The graph exhibits once again that the interference-induced narrow spectral lines will be widened and reduced if the linewidth of the driving laser is taken into account. For large laser linewidths, for example, $L=5\gamma$, the sharp peak will disappear (not shown here).

V. CONCLUSION

We have shown that the resonance fluorescence spectrum of a driven V atom is greatly modified by quantum interfer-

ence between the two transition pathways from the excited doublet to the common ground level. For the case of the degenerate excited doublet, the spectrum exhibits a Mollow-like triplet. Radiative interference always broadens the spectral lines. However, more interesting phenomena due to quantum interference emerge in the situation in which the excited doublet is nondegenerate. The fluorescent emission can be completely suppressed if the atomic dipole moments are parallel (which maximizes quantum interference) and the coherent field is tuned to the average frequency of the atomic transitions. Otherwise, significant spectral narrowing at line center takes place over a wide range of parameters, for parallel or nearly parallel dipole transition moments. If the laser linewidth is taken into account the atom can be never trapped in a dressed state, so that no fluorescence quenching displays. Nevetheless, the spectral lines can still be significantly narrowed provided the laser linewidth does not greatly exceed the natural width.

These effects have a straightforward interpretation in the dressed-state representation. The quantum interference between the two transition pathways can drive the atom into a dressed state that is decoupled from the fields, preventing any fluorescence, although population inversion is achieved when the coherent field is tuned to the average frequency of the atomic transitions. The dressed state decays very slowly for small excited doublet splittings for nearly maximum quantum interference. It is the slow decay that gives rise to the striking narrow spectral profile at line center. The width of the narrow spectral line is proportional to the square of the ratio of the level splitting to the effective Rabi frequency and may thus be very narrow for small splittings.

ACKNOWLEDGMENTS

The authors wish to thank V. Buzek, E. Arimondo, and M. Plenio for conversations on quantum interference and J. C. Camparo, P. L. Knight, and S. Y. Zhu for providing us with copies of their work prior to publication. This work was supported by the United Kingdom EPSRC, by the EC, and by NATO.

[1] E. Arimondo, in *Progress in Optics XXXV*, edited by E. Wolf (Elsevier, Amsterdam, 1966), p. 257.

[2] P. Meystre and M. Sargent III, *Elements of Quantum Optics* (Springer-Verlag, Berlin, 1991); G. C. Hegerfeldt and M. B. Plenio, Phys. Rev. A **47**, 2186 (1993); Quantum Opt. **6**, 15 (1994); B. M. Garraway and P. L. Knight, Phys. Rev. A **54**, 3592 (1996).

[3] S. Y. Zhu, R. C. F. Chan, and C. P. Lee, Phys. Rev. A **52**, 710 (1995).

[4] P. Zhou and S. Swain (unpublished).

[5] T. Hellmuth, H. Walther, A. Zajonc, and W. Schleich, Phys. Rev. A **35**, 2532 (1987); V. Langer, H. Stolz, and W. von der Osten, Phys. Rev. Lett. **64**, 854 (1990).

[6] G. S. Agarwal, in *Quantum Optics*, Springer Tracts in Modern Physics Vol. 70 (Springer-Verlag, Berlin, 1974).

[7] P. Zhou and S. Swain, Phys. Rev. Lett. **78**, 832 (1997).

[8] D. A. Cardimona, M. G. Raymer, and C. R. Stroud, Jr., J. Phys. B **15**, 65 (1982).

[9] M. O. Scully, S. Y. Zhu, and A. Gavrielides, Phys. Rev. Lett. **62**, 2813 (1989).

[10] G. C. Hegerfeldt and M. B. Plenio, Phys. Rev. A **46**, 373 (1992).

[11] P. Zhou and S. Swain, Phys. Rev. Lett. **77**, 3995 (1996).

[12] S. E. Harris, Phys. Rev. Lett. **62**, 1033 (1989); S. E. Harris and J. J. Macklin, Phys. Rev. A **40**, R4135 (1989); A. Imamoglu, *ibid.* **40**, R2835 (1989); M. Fleischhauer, C. H. Keitel, L. M. Narducci, M. O. Scully, S. Y. Zhu, and M. S. Zubairy, Opt. Commun. **94**, 599 (1992).

[13] S. Y. Zhu and M. O. Scully, Phys. Rev. Lett. **76**, 388 (1996); S. Y. Zhu, Quantum Opt. **7**, 385 (1995); H. Huang, S. Y. Zhu, and M. S. Zubairy, Phys. Rev. A **55**, 744 (1997); H. Lee, P. Polynkin, M. O. Scully, and S. Y. Zhu, *ibid.* **55**, 4454 (1997).

[14] H. R. Xia, C. Y. Ye, and S. Y. Zhu, Phys. Rev. Lett. **77**, 1032 (1996).

[15] G. S. Agarwal, Phys. Rev. A **55**, 2457 (1997).

[16] S. Y. Zhu, L. M. Narducci, and M. O. Scully, Phys. Rev. A **52**, 4791 (1995); A. H. Toor, S. Y. Zhu, and M. S. Zubairy, *ibid.* **52**, 4803 (1995); S. Y. Zhu and M. O. Scully, Phys. Lett. A **201**, 85 (1995).

[17] G. S. Agarwal, Phys. Rev. A **55**, 2467 (1997).

[18] G. Alzetta, A. Gozzini, L. Moi, and G. Orriols, Nuovo Cimento B **36**, 5 (1976); S. E. Harris, J. E. Field, and A. Imamoglu, Phys. Rev. Lett. **64**, 1107 (1990); K. Hakuta, L. Marmet, and B. P. Stoicheff, Phys. Rev. A **45**, 5152 (1992); S. E. Harris, Phys. Rev. Lett. **70**, 552 (1993); **72**, 52 (1994); J. Gea-Banacloche, Y. Li, S. Jin, and M. Xiao, Phys. Rev. A **51**, 576 (1995); S. E. Harris and Z. F. Luo, *ibid.* **52**, R928 (1995); D. J. Fulton, S. Shepherd, R. R. Mosely, B. D. Sinclair, and M. H. Dunn, *ibid.* **52**, 2302 (1995).

[19] O. Kocharovskaya and Ya. I. Khanin, Pis'ma Zh. Eksp. Teor. Fiz. **48**, 581 (1988) [JETP Lett. **48**, 630 (1988)]; A. Imamoglu, J. E. Field, and S. E. Harris, Phys. Rev. Lett. **66**, 1154 (1991); G. S. Agarwal, *ibid.* **67**, 980 (1991); Phys. Rev. A **44**, R28 (1991); L. M. Narducci, H. M. Doss, P. Ru, M. O. Scully, S. Y. Zhu, and C. Keitel, Opt. Commun. **81**, 379 (1991); L. M. Narducci, M. O. Scully, C. Keitel, S. Y. Zhu, and H. M. Doss, *ibid.* **86**, 324 (1991); O. Kocharovskaya, Phys. Rep. **219**, 175 (1992), and references therein; Y. Zhu, Phys. Rev. A **45**, R6149 (1992); K. K. Meduri, G. A. Wilson, P. B. Sellin, and T. W. Mossberg, Phys. Rev. Lett. **71**, 4311 (1993); C. Keitel, O. Kocharovskaya, L. M. Narducci, M. O. Scully, and S. Y. Zhu, Phys. Rev. A **48**, 3196 (1993); G. S. Agarwal, G. Vemuri, and T. W. Mossberg, *ibid.* **48**, R4055 (1993); G. A. Wilson, K. K. Meduri, P. B. Sellin, and T. W. Mossberg, *ibid.* **50**, 3394 (1994); G. Grynberg, M. Pinard, and P. Mandel, *ibid.* **54**, 776 (1996).

[20] M. O. Scully, Phys. Rev. Lett. **67**, 1855 (1991); M. Fleischhauer, C. H. Keitel, M. O. Scully, C. Su, B. T. Ulrich, and S. Y. Zhu, Phys. Rev. A **46**, 1468 (1992); M. O. Scully and S. Y. Zhu, Opt. Commun. **87**, 134 (1992); M. O. Scully, Phys. Rep. **219**, 191 (1992), and references therein.

[21] G. S. Agarwal, Phys. Rev. A **54**, R3734 (1996).

[22] L. M. Narducci, M. O. Scully, G. L. Oppo, P. Ru, and J. R. Tredicce, Phys. Rev. A **42**, 1630 (1990); A. S. Manka, H. M. Doss, L. M. Narducci, P. Ru, and G. L. Oppo, *ibid.* **43**, 3748 (1991).

[23] D. J. Gauthier, Y. Zhu, and T. W. Mossberg, Phys. Rev. Lett. **66**, 2460 (1991).

[24] H. R. Gray, R. M. Whitely, and C. R. Stroud, Jr., Opt. Lett. **3**, 218 (1978); G. Orriols, Nuovo Cimento B **53**, 1 (1979); R. P. Hackel and S. Ezekiel, Phys. Rev. Lett. **42**, 1736 (1979); M. Kaivola, P. Thorsen, and O. Poulsen, Phys. Rev. A **32**, 207 (1985); K. Hakuta, L. Marmet, and B. P. Stoicheff, Phys. Rev. Lett. **66**, 596 (1991); K. J. Boller, A. Imamoglu, and S. E. Harris, *ibid.* **66**, 2593 (1991); J. E. Field, K. H. Hahn, and S. E. Harris, *ibid.* **67**, 3062 (1991); A. Kasapi, M. Jain, G. Y. Yin, and S. E. Harris, *ibid.* **74**, 2447 (1995); M. Xiao, Y. Li, S. Jin, and J. Gea-Banacloche, *ibid.* **74**, 666 (1995); Y. Li and M. Xiao, Phys. Rev. A **51**, R2703 (1995); **51**, 4959 (1995); R. R. Mosely, S. Shepherd, D. J. Fulton, B. D. Sinclair, and M. H. Dunn, Phys. Rev. Lett. **74**, 670 (1995).

[25] A. S. Zibrov, M. D. Lukin, D. E. Nikonov, L. Hollberg, V. L. Velichansky, and H. G. Robinson, Phys. Rev. Lett. **75**, 1499 (1975); G. G. Padmabandu, G. R. Welch, I. N. Shubin, E. S. Fry, D. E. Nikonov, M. D. Lukin, and M. O. Scully, *ibid.* **76**, 2053 (1996); P. B. Sellin, G. A. Wilson, K. K. Meduri, and T. W. Mossberg, Phys. Rev. A **54**, 2402 (1996).

[26] J. C. Camparo and P. Lambropoulos, Phys. Rev. A **55**, 552 (1997).

[27] K. Banaszek and P. L. Knight, Phys. Rev. A **55**, 2368 (1997).

[28] N. Ph. Georgiades, E. S. Polzik, and H. J. Kimble, Opt. Lett. **21**, 1688 (1996); Phys. Rev. A **55**, R1605 (1997); S. R. Wilkinson, A. V. Smith, M. O. Scully, and E. Fry, *ibid.* **53**, 126 (1996).

[29] P. Zhou and S. Swain, Phys. Rev. A **54**, 2455 (1996); Opt. Commun. **134**, 127 (1997).

[30] V. Buzek, Phys. Rev. A **39**, 2232 (1989).

[31] G. C. Hegerfeldt and M. B. Plenio, Phys. Rev. A **52**, 3333 (1995); M. B. Plenio, J. Mod. Opt. **43**, 753 (1996); Z. Phys. D **96**, 533 (1995).

[32] B. M. Garraway, M. S. Kim, and P. L. Knight, Opt. Commun. **117**, 560 (1995).

[33] H. G. Dehmelt, Bull. Am. Phys. Soc. **20**, 60 (1975); R. J. Cook and H. J. Kimble, Phys. Rev. Lett. **54**, 1023 (1985).

[34] M. Fleischauer, C. H. Keitel, L. M. Narducci, M. O. Scully, S.-Y. Zhu, and M. S. Zubairy, Opt. Commun. **94**, 599 (1992).

[35] P. Zhou and S. Swain, Opt. Commun. **123**, 297 (1996).

[36] D. F. Walls and G. J. Milburn, *Quantum Optics* (Springer, Berlin, 1994).

[37] M. Lax, Phys. Rev. **172**, 350 (1968); S. Swain, J. Phys. A **14**, 2577 (1981).

[38] C. Cohen-Tannoudji and S. Reynaud, J. Phys. B **10**, 345 (1977); in *Multiphoton Processes*, edited by J. H. Eberly and P. Lambropoulos (Wiley, New York, 1978); T. A. B. Kennedy and S. Swain, Phys. Rev. A **36**, 1747 (1987).

[39] B. R. Mollow, Phys. Rev. **188**, 1969 (1969).

[40] C. R. Fu, Y. M. Zhang, and C. D. Gong, Phys. Rev. A **45**, 505 (1992).

[41] G. S. Agarwal, Phys. Rev. A **18**, 1490 (1978); K. I. Osman and S. Swain, J. Phys. B **13**, 2397 (1980); G. S. Agarwal, C. V. Kunasz, and J. Cooper, Phys. Rev. A **36**, 5654 (1987); S. Smart and S. Swain, *ibid.* **45**, 6863 (1992); S. Sultana and M. S. Zubairy, *ibid.* **49**, 438 (1994); A. H. Toor, S. Y. Zhu, and M. S. Zubairy, *ibid.* **52**, 4803 (1995).